

**Trace element concentrations of ilmenite in samples selected from the six Apollo landed missions.** C.-E. Morisset<sup>1</sup>, Jackson, S.<sup>2</sup>, Williamson, M.-C.<sup>2</sup> and Hipkin, V. J.<sup>1</sup>, <sup>1</sup>Canadian Space Agency, 6767 route de l'Aéroport (Saint-Hubert) Québec J3Y 8Y9, e-mail: [caroline-emmanuelle.morisset@asc-csa.gc.ca](mailto:caroline-emmanuelle.morisset@asc-csa.gc.ca), <sup>2</sup>Geological Survey of Canada, 601 Booth Street, Ottawa K1A 0E8.

**Introduction:** We report the trace element concentrations of ilmenite contained in twelve samples selected from the six Apollo landing sites using a Laser-Ablation – Inductively Coupled Plasma – Mass Spectrometer (LA-ICP-MS). Oxygen is a key lunar resource and ilmenite is the best candidate for oxygen extraction amongst minerals present in the regolith due to the fact that oxygen can be liberated at lower temperature in the ilmenite (1000°C [1]) than in silicates (at least 1100°C [2]). Ilmenite modal abundances can reach up to 25% in mare basalts, and up to 9% in lunar regolith [3].

With a new set of trace element analyses in lunar ilmenite, we will: (1) determine the concentrations of harmful elements that should be monitored during oxygen production (e.g. Pb, Cd); (2) provide a new set of geochemical data complementary to the existing lunar datasets on ilmenite (e.g. [4, 5, 6]); and (3) compare the new data with terrestrial ilmenite compositions to understand the role of this important mineral in magmatic processes during the formation of the Earth and the Moon. These might be different because terrestrial ilmenite contains Fe<sup>3+</sup> that facilitates the substitutions of 3+ cations whereas lunar ilmenite does not. We present some preliminary results on five of the selected samples. Analyses of the remaining seven samples are ongoing. We anticipate that a complete set of results for this project will contribute significantly to our current understanding of the science and engineering requirements for In Situ Resource Utilization (ISRU), and ultimately refine our knowledge of the geological evolution of the Moon.

#### Method:

**Sample selection.** Twelve thick sections (two for each Apollo mission), have been selected for the study. The samples were chosen from each of the Apollo landed missions in order to study the ilmenite compositions over the greatest possible geographical area. Ten of the requested sections are from basalt samples (10024, 10050, 12005, 12021, 14053, 14072, 15016, 15536, 70017, and 71037), one is from an impact melt breccia sample (65015), and one is from an impact melt sample (68416). We selected a range of different rock types in order to assess the variability of the trace element compositions of ilmenite. Other selection criteria included the size of ilmenite grains (minimum 50 µm) and availability of an absolute age.

**Analyses.** The thick sections were first imaged with a Scanning Electron Microscope (SEM) (Cambridge S-360) at the Geological Survey of Canada (GSC) in Ottawa to select ilmenite grains that were best suited for trace element analyses (e.g. grains that have an area larger than 50 µm free of cracks and inclusions). The samples were then analyzed by Electron Microprobe (CAMECA SX-100) at the Université Laval in Québec City. Ti (along with Fe, Mg, Al, Cr, Mn, and Zr) was measured so it could be used as an internal standard for the LA-ICP-MS analyses. Finally, the ilmenite grains were analyzed by LA-ICP-MS using a Photon-Machines Analyte 193 laser and an Agilent 7500 ICP-MS at the GSC in Ottawa. About 70 elements from Li to U were initially measured to determine which elements were present in concentrations high enough to be detected. After looking at the results for 10 analyses or more for each sample, a subgroup of 50 elements was selected for the next round of analyses. Up to 26 spots on 18 ilmenite grains were analyzed per thick section.

#### Results:

**Oxide textures.** The optical microscopy and SEM imaging enabled the identification of rutile needles in some ilmenite grains in five of the basalt samples (Fig. 1a). Chromium-rich spinel needles were found to be associated with the rutile needles in three of these samples (Fig. 1a). Baddeleyite blebs and needles were found in ilmenite grains from six basalt samples (Fig. 1b) and in sample 68416.

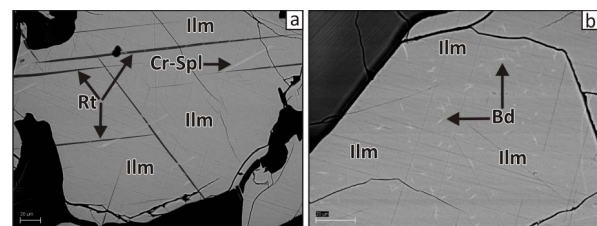


Figure 1. Back-Scattered electron images showing detailed mineralogy of thick section 70017, 557. (a) Rutile (Rt) and chromium-rich spinel (Cr-Spl) needles in the ilmenite (Ilm). (b) Baddeleyite (Bd) needles and blebs in the ilmenite.

**Major and trace elements.** Five of the twelve thick sections have been analyzed with EPMA (10024, 110; 12005, 68; 12021, 601; 14053, 286; and 70017, 557) and three of those have been analyzed with LA-ICP-

MS (10024, 110; 12021, 601; and 70017, 557). The  $\text{TiO}_2$  wt% in the analyzed ilmenite varies from 52.9 to 55.9 ( $2\sigma$  is 0.4 wt%); the FeO wt% from 38.6 to 46.4 ( $2\sigma$  is 0.6 wt%); and the MgO wt% from 0.1 to 5.1 ( $2\sigma$  is 0.1 wt%). The MgO wt% of the ilmenite grains from sample 70017, 557 ranges from 1.7 to 5.0 (Fig. 2) while the largest variation within a grain is of 0.2 (e.g. 2.6-2.8 MgO wt%) implying that the observed variation between grains cannot be attributed to mineral zoning. Cr varies from 944 to 6958 ppm, Mn from 256 to 3275 ppm, and V from 80 to 454 ppm. A positive correlation is observed between MgO wt% and  $\text{TiO}_2$  wt% (Fig. 2) and between MgO wt% and Cr while a negative correlation is observed between MgO wt% and FeO wt%. Zr (123-2327 ppm) and Hf (5.95-85 ppm) concentrations are highest in the baddeleyite-bearing ilmenite grains. Nb (20-107 ppm) and Ta (1.85-8.52 ppm) are positively correlated but are not well correlated with Zr or Hf. Finally, REE patterns are enriched in HREE (Lu: 0.29-4.85 ppm) with a strong Eu negative anomaly (Eu/Eu\* from 0.003 to 0.413) (Fig. 3).

Concentrations of harmful elements are low or below detection limits (e.g. Cd from below detection to 0.27 ppm; Pb from below detection to 1.5 ppm).

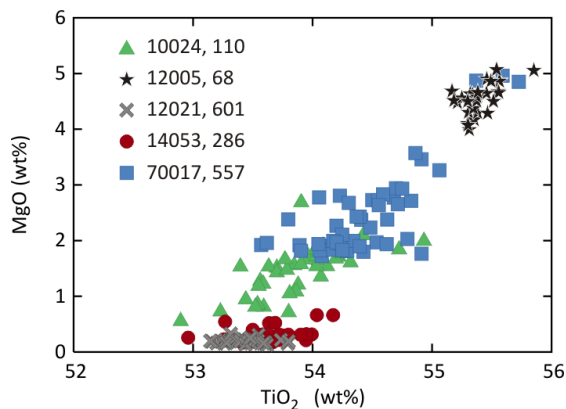


Figure 2. MgO (wt%) versus  $\text{TiO}_2$  (wt%) for ilmenite from five thick sections analyzed with Electron Microprobe showing a positive correlation between the two components.

**Discussion:** The presence of the rutile and chromium-rich spinel needles in ilmenite (Fig. 1a) can be explained by the production of rutile + spinel + Fe + O as the result of a reduction reaction of ilmenite (e.g. [7]). Also, the negative trend between MgO wt% and FeO wt% is expected because Mg substitutes for  $\text{Fe}^{2+}$  in the ilmenite. However, the positive trend between MgO wt% and  $\text{TiO}_2$  wt% and the fact that there is almost no overlap in MgO wt% analyzed in the ilmenite grains from the various samples is intriguing (Fig. 2).

The range of MgO wt% values within the ilmenite grains of a single sample of basaltic rock (i.e. 70017, 557, Fig. 2) must be accounted for. There is a negative correlation between the Lu (0.29-4.85 ppm) and the MgO concentrations of the ilmenite grains in sample 70017, 557, that could be attributed to fractional crystallization. Unlike MgO, Lu is an incompatible element in a basaltic system implying that the ilmenite with the highest MgO content crystallized first. Fractional crystallization modeling will enable us to assess whether this process can reproduce the observed trend. We will then need to evaluate how ilmenite grains showing an important fractional crystallization trend can occur in the same basalt sample.

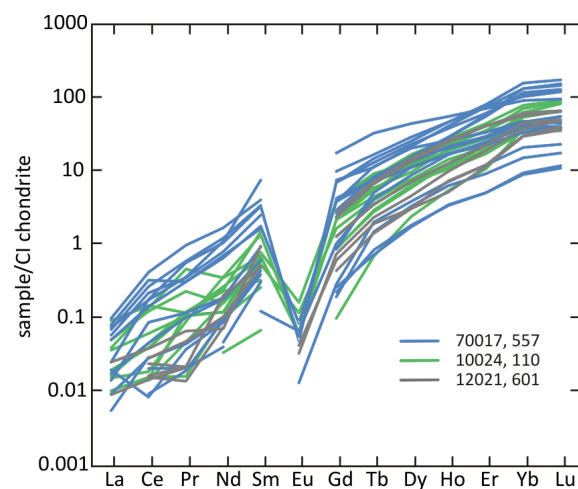


Figure 3. CI chondrite-normalized REE diagram of representative ilmenite analyses from three thick sections analyzed with LA-ICP-MS. CI chondrite-normalizing values from [8].

**References:** [1] Gibson M. A. and Knudsen C. W. (1985) Mendell W. W. (ed) *Lunar Bases and Space Activities of the 21<sup>st</sup> Century*, pp. 543-550. [2] Kesterke S. (1971) U.S. Bureau of Mines Report of Investigations 7587, 12 p. [3] McKay D. S. and Williams R. J. (1979) *Space Resources and Space Settlements*, pp 243-255. [4] Haggerty S. E. et al. (1970) *Science* 167, 613-615. [5] El Goresy A. et al. (1971) *Earth Planet. Sci. Lett.* 13, 121-129. [6] Papike J. et al. (1993) Heiken G.H., Vaniman D.T. and French B. M. (eds) *The Lunar Sourcebook, a user's guide to the Moon*, pp 121-181. [7] El Goresy A. and Ramdohr P. (1975) *Proc. Lunar Sci. Conf. VI*, 245-247. [8] McDonough W. F. and Sun S. S. (1995) *Chem. Geol.* 120, 223-253.